View metadata, citation and similar papers at core.ac.uk
brought to you by CORE
provided by Heriot Watt Pure

Laser Sintering of Nano-Ag Particle Paste for High Temperature Electronics Assembly

Wei Liu, Changhai Wang *Member*, *IEEE*, Chunqing Wang, Xin Jiang and Xi Huang

***Abstract*—In this paper we have investigated a laser-assisted fast nano-Ag sintering process for die-attach in power electronic applications. The effects of laser power, irradiation time and load on microstructure and shear performance of the bonded samples are presented. Moreover, samples sintered by a hotplate were also studied as a comparison. The results indicate that the die-attach process using the nano-Ag material can be realized within 1 min in the laser-assisted sintering method. In general better shear strength was obtained with increasing laser power, irradiation time and load. The shear strength of samples irradiated by 2 – 5 minutes of laser beam was comparable to that of the samples sintered on the hotplate for 80 minutes.**

***Index Terms*— laser sintering, silver nanoparticle paste, die-attach.**

I. Introduction

With the increase in power density of electronic products, especially for the next generation semiconductor devices, such as SiC or GaN devices, dies within the devices will be operated at temperatures higher than 200°C, and in some cases even operating at 600°C [1-3]. As a result, the traditional die-attach materials, such as Sn-based solders and adhesives, are not suitable for these devices since the materials cannot withstand the harsh operation environment, and it is a bottleneck for the development of high power electronic devices. Therefore, it is necessary to develop new die-attach materials and processes in order to realize application of high power electronic devices [4-5].

Recently, nano-Ag particles have attracted much attention because silver has better thermal and electrical conductivity than that of the commonly used Sn-Pb or Pb-free solders. Moreover, nano-Ag particles can be sintered below 200°C, and once they are sintered to form a joint, the material will have a melting temperature similar to that of the bulk silver (961°C). Due to this property nano-Ag particles have become a promising candidate for die-attach applications in high power electronic devices [6-10]. However, sintered nano-Ag joints have porous structures [11-12]. In order to densify the microstructures and increase the strength of nano-Ag joints, the effects of sintering time, temperature and pressure have been studied, such as increasing sintering time from 30 mins to several hours, elevating sintering temperature to 400°C and increasing sintering pressure to 10 MPa [13]. It has been shown that such approaches can improve the density and strength of nano-Ag joints. However, the long sintering time reduces the manufacturing efficiency of electronic products, and high sintering temperature and pressure will increase the risk of damage to the chip and the substrates of electronic devices. Another approach for densifying microstructures of nano-Ag joints is to use the same nanometer diameter Ag particles of several nanometers in diameter [14]. Such nano-Ag particles can be sintered at very low temperatures, even at room temperature [15-16]. However, it is more expensive to manufacture such superfine particles and the increased material cost will hinder the application of the superfine nano-Ag particles. Therefore a more cost-effective route would be to explore nano-Ag materials consisting of nanometer Ag particles and micron or submicron Ag particles to take advantages of the low material cost and low sintering temperature. However, there has been little study of the sintering behavior and process parameters for such materials.

In the conventional sintering processes the same temperature is applied to the dies, components, substrates and bonding materials and has several drawbacks, such as long process time, low heating rate and global heating (not suitable for electronic systems with components sensitive to high temperature). As an alternative approach, the laser-assisted sintering technique can be used to realize localized sintering of the nano-Ag paste material by using the selective laser heating effect. Hence, the laser beam will only affect the target area, and will not cause heat induced damage to temperature sensitive components during the sintering process [17-19]. Jiang et al. have realized line bonding for microsystem packaging by using a transmission laser bonding technique [17]. Moreover, the laser based method has a unique characteristic of high power density and the laser irradiation time can be controlled precisely [20-21]. Tian et al. have bonded sensor pad and substrate using solder balls (100 µm in diameter) using a laser based method and showed that the laser irradiation time can be controlled to be within 10 ms [21]. Therefore, by controlling the laser beam intensity and irradiation time, it is possible to realize rapid laser sintering of nano-Ag particles for die-attach applications. At present, this

Wei Liu, Chunqing Wang and Xi Huang are with State Key Laboratory of Advanced Welding and Joining, Harbin Institute of Technology, Harbin, 150001, China (e-mail: w_liu@hit.edu.cn; wangcq@hit.edu.cn; huangxi2015 @hotmail.com)
Changhai Wang is with Institute of Sensors, Signals and Systems, School of Engineering and Physical Sciences, Heriot-Watt University, Edinburgh, EH14 4AS, UK (e-mail: c.wang@hw.ac.uk)
Xin Jiang was with the Heriot-Watt University, he is with Semiconductor Manufacturing International Corporation, 18 Zhangjiang Road, Shanghai, China (email: xin_jiang@smics.com)

technique has been utilized to sinter inkjet-printed nano-particle films or patterns on different substrates [22-25]. Lee et al. have sintered a silver nanoparticle ink within 60 s using a 532 nm continuous wave laser [24]. They have also demonstrated a die attach process for 1.5×1.5 mm^2 high power LED chips by laser sintering of a nano-Ag paste [26]. However, little literature has reported investigation of the laser-assisted sintering technique for die-attach for power electronic applications using nano-Ag pastes and large size chips or dies. Moreover, studies of microstructures and the mechanical performance of the laser sintered samples are also necessary.

In this paper, we have studied a laser-assisted nano-Ag sintering process for bonding of Si substrates. The microstructure, shear strength and surfaces after fracture of the nano-Ag bonded samples have been investigated for different laser processing conditions.

II. Experimental section

A. Nano-Ag Paste Material, Printing and Drying

The nano-Ag paste (NanoTach®-X) used in this study was obtained from NBE Technologies, LLC. The material consisted of 30 nm to 50 nm silver nano-particles and some micron-sized Ag particles mixed in an organic solvent/binder system. Fig. 1 shows the appearance of the nano-Ag paste after treatment at 110℃ for 5 min. Si wafers were used in this study to fabricate substrates. The Si wafers were 600 µm in thickness and coated with titanium and copper films of thicknesses of 200 nm and 600 nm respectively. The metal films were deposited by electron-beam evaporation. The wafers were then diced to obtain substrates of 5x5 mm^2 or 10x10 mm^2 using a diamond saw and then cleaned for printing of nano-Ag paste layer and for laser sintering experiments. The smaller silicon substrates are also referred to as dies.

The samples for sintering were prepared in the following process: the nano-Ag paste was printed onto the 10x10 mm^2 silicon substrates using a steel stencil. The aperture size of the steel stencil was 5x5 mm^2 and the thickness was 100µm. Fig. 2 shows the appearance and measured thickness profile of the printed nano-Ag paste layer. In the central part of the printed nano-Ag paste layer, the thickness was about 95 µm.

B. Hotplate Based Sintering Method

A hotplate based sintering process was carried out to obtain bonded samples of silicon substrates. The smaller silicon substrate (5x5 mm^2) was aligned to the printed nano-Ag layer on the larger substrate and then bonded together by thermal sintering of the nano-Ag layer on the hotplate. The samples were used for comparison with the laser sintered counterparts. Two temperature profiles were used in this study. The first profile consisted of 6 dwell stages, 60℃, 100℃, 140℃, 180℃, 220℃ and 260℃ respectively. The ramp rate was 0.3℃/s. The dwelling time for the first 5 stages was 7 min at each set temperature, and the dwelling time at the last stage (260℃) was 30 min. After sintering the temperature of the hotplate was decreased from 260℃ to 50℃ in 15 min. The second profile also included 6 dwell stages, the only difference was that the temperature of the last dwelling stage was 285℃. In all of the hotplate based sintering work, a 0.1 kg Cu load was applied to the substrate assembly through an intermediate circular glass plate.

C. Laser Based Sintering Method

A schematic drawing of the laser-assisted sintering setup is shown in Fig. 3. Prior to the laser-assisted sintering process, all the samples were pre-bonded on the hotplate using the same configuration as for the hotplate based sintering work and the same load of 0.1 kg but only one dwelling stage at 110℃ for 5 min. A high-power diode laser system with a fiber-coupled output at 970 nm was used in this work. The laser output from the beam delivery fiber was transformed into a square beam with top-hat intensity distribution. The beam profile was produced using a custom-designed beam forming optical element [27]. The beam size was 6x6 mm^2. The beam transmission module consists of collimation optics followed by a focusing lens with a focal length of 20 cm. The sample for sintering was placed on a precision translation stage. A ceramic plate with a thickness of 0.9 mm was placed under the substrate assembly to reduce thermal loss into the stainless steel platform [28]. For laser sintering, the nano-Ag layer between the Si substrates was aligned to the laser beam. A copper load of 0.1 kg or 0.5 kg was applied to the top silicon substrate through an intermediate glass plate. The sintering processes were all carried out under the atmospheric environment. The laser beam was passed through the aperture of the copper plate based load and then the intermediate glass plate to reach to the top silicon chip. The incident laser power, after reflection loss from the silicon surface, was all absorbed by the top silicon substrate. The thermal power from the absorbed laser beam produces a sufficient temperature in the nano-Ag film to result in thermal sintering of the nano-Ag layer and bonding of the two silicon substrates. The laser power of 60 W or 70 W was used in the experiments and the laser irradiation time was 1, 2 or 5 minutes.

D. Shear Test and Studies of Microstructures

Shear test was carried out on an Instron 5569 system to determine the shear strength of the bonded silicon substrates by sintering of the intermediate nano-Ag layer. The shear speed in the test was set as 0.5 mm/min. The average value of the test results was obtained from five samples processed under the same conditions in order to evaluate the mechanical strength of the joints. After the shear test, the surfaces of the substrates were analyzed by SEM and EDX to identify fracture modes and locations. To study the microstructures of the nano-Ag joints sintered by different processes, selected samples were mounted in epoxy resin, and then sectioned perpendicular to the planes of the substrates to obtain cross-sections for analysis. The cross-sectional surfaces were grinded and polished. Scanning Electron Microscopy (SEM) was used to analyze the microstructures of the sintered joints.

III. Results and discussion

A. Shear Test

1) Shear Strength

Table 1 shows the results of shear strength of the samples sintered by both the laser and hotplate based methods and the

associated parameters. The shear strengths of the samples sintered by hotplate with the maximum dwelling temperature of 260℃ and 285℃ are 4.79 and 4.64 MPa respectively. There is not much difference between the values of the shear strength. For the laser sintered samples, the average shear strength of the samples was 4.43 MPa under the conditions of 60 W for laser power, 2 min for irradiation time and 0.1 kg for load. The shear strength was comparable to the samples sintered on the hotplate. When the laser irradiation time was increased to 5 min, the shear strength of the samples was 5.11 MPa, which is higher than that of the samples sintered by the hotplate. As the laser power was increased to 70 W and the irradiation time was reduced to 1 min, the shear strength of the samples decreased to 1.89 MPa. When the Cu load of 0.5 kg was used, the shear strength of the samples sintered at the laser power of 70 W was improved to 2.08 and 5.54 MPa respectively for the corresponding irradiation time of 1 min and 5 minutes.

The results indicate that fast sintering of nano-Ag particles can be achieved using the laser assisted approach. Better shear strength can be obtained using higher laser power and hence the sintering temperature, longer irradiation time and more load. Moreover, the shear strength of the samples produced at the laser sintering time of 2 to 5 min is comparable and even higher than the samples sintered on hotplate for 80 minutes.

2) Fracture Analysis after Shear Test

Fig. 4 shows the pictures of fracture surfaces of the hotplate sintered samples based on the two different temperature profiles. The samples sintered at the final dwelling temperature of 260°C or 285°C showed a similar fracture mode. Most of the fracture surfaces were from the interface between the sintered nano-Ag layer and the Cu films on silicon substrates. Some Ag particles/fragments can be seen on the surface of the Cu films, but most of the Cu surfaces were not covered by the residues of the sintered Ag layer.

Fig. 5 shows the fracture surfaces of the samples sintered with 0.1 kg of load and 60 W of laser power for different irradiation times. For the samples sintered for 2 minutes of laser irradiation, the fractures were mostly located at the interface of the sintered Ag layer and the Cu film. A significant amount of Ag particles could be observed on the Cu surface, and the size of the Ag particles was smaller than those shown in Fig. 4. Moreover, cracks were observed within the sintered Ag layer. In Fig. 5(b), as the laser irradiation time was increased to 5 min, more fractures appeared in the sintered Ag layer.

Fig. 6 shows fractures of samples sintered using 70 W of laser power with two different loads of 0.1 kg and 0.5 kg and irradiation times of 1 and 5 minutes respectively. For 0.1 kg of load and 1 min of laser irradiation, some fractures were located within the sintered Ag layer, and the other fractures occurred at the interface of the sintered Ag layer and the Cu film. When the load was 0.5 kg (Fig. 6(b)), more fractures were found from the sintered Ag layer as compared with those in Fig. 6(a). At the load of 0.5 kg and 5 min of laser irradiation, the fractures are in mixed mode: within sintered Ag layer and at the interface between the sintered Ag layer and the Cu films.

B. Cross-Sectional Studies

Fig. 7 shows optical pictures of the cross-sections of a sample sintered on hotplate and by laser irradiation. As for the sample sintered on hotplate with the maximum dwelling temperature of 260℃ (Fig. 7(a)), the total time of the sintering process was 80 min as stated previously. In Fig. 7(b), the cross-section was from a sample sintered using 60 W of laser power for 5 minutes. The applied load was 0.1 kg in the sintering process. The pictures show that both the hotplate and laser-assisted sintering processes can produce samples with uniform and continuous nano-Ag sintered joints.

1) Hotplate Sintering

Fig. 8 shows the cross-sections of two samples sintered on hotplate at different maximum dwelling temperatures. As can be seen in Fig. 8(a), when the maximum dwelling temperature was 260℃, nano-Ag particles formed a network Ag structure with many voids after sintering. Most of the Ag layer formed a joint with the copper films and only a few unbonded areas can be seen at the interfaces. The length of the unbonded areas along the interface is up to 2 μm. As the maximum temperature of the sintering process was increased to 285℃, the central part of the joint became denser than that of the sample sintered at the maximum temperature of 260℃. However, some large voids formed near the interface of the Ag layer and the copper films and the length of the voids is as large as 5 μm.

The results indicate that in most of the samples sintered on hotplate a coarsened network of Ag structure was formed. Moreover, the degree of coarsening may be increased with the sintering temperature. Most fractures of the samples occurred at the interfaces of the sintered Ag layer and the Cu films. This behavior indicates that the Ag and Cu interfaces were the weak bonding locations for the samples sintered on hotplate. The reason may be that the samples were sintered in ambient atmosphere and the Cu films could be oxidized during the prolonged sintering process.

2) Laser Sintering

Fig. 9 shows the cross-sections of samples sintered at the laser irradiation of 60 W and 0.1 kg of load. For the laser irradiation time of 2 min, fine network Ag structures were formed in the nano-Ag layer. Most of the voids were about or less than 1 μm in length. Moreover, the microstructures are uniform. When the laser irradiation time was increased to 5 min, coarsened networks of Ag structures were formed. The sizes of voids were also increased, but evenly distributed within the Ag joint. At the interfaces of the Ag layer and the Cu films, the length of the unbonded areas was about 3 μm.

Fig. 10 shows the cross-sections of samples sintered at the laser power of 70 W and the load of 0.1 kg or 0.5 kg for different irradiation times. As shown in Fig. 10(a), in the case of the laser irradiation time and load of 1 min and 0.1 kg, coarsened networks of Ag structures were formed within the nano-Ag joint showing large voids. Many of the voids were longer than 2 μm. In Fig. 10(b), when the laser irradiation time and load were 1 min and 0.5 kg, dense networks of Ag structures were formed and only small voids could be seen within the joint. Moreover, there are fewer voids formed at the interface of the Ag layer and the Cu films. As shown in Fig. 10(c), when the laser irradiation time of 5 min and load of 0.5

kg were applied, the joint became denser than that shown in Fig. 10 (b). The number of voids also decreased indicating the formation of good bond between the sintered Ag layer and the Cu films on the silicon substrates.

The results of the cross-sectional study indicate that it is possible to realize laser assisted sintering of the nano-Ag particle paste layer within 1 min for die-attach applications. With the increase of laser irradiation time and power, coarsened Ag structures would form. When the load was increased during the sintering process, the microstructures of the nano-Ag layer were densified. Even the samples were sintered by different laser irradiation parameters, the network structures in the Ag layers were all quite uniform. Under the conditions of high laser power, long laser irradiation and large Cu load, most of the samples showed mixed fracture mode: within the sintered Ag layer and at the interface of sintered Ag and Cu films. This phenomenon indicates that the bonding strength of the sintered Ag layer and the bonding strength with the Cu films were all enhanced in the laser assisted sintering process.

The microstructures and shear performance of the laser sintered joints depend on the temperature profile applied to the nano-Ag particle paste and Cu films. Fig. 11 shows the temperature profiles monitored by a thermocouple in the laser sintering process. For temperature monitoring, the thermocouple was placed below the silicon substrate assembly and aligned to center of the nano-Ag pattern on the bottom Si substrate. Although the monitored temperature was expected to be lower than the temperature in the nano-Ag layer due to the effect of temperature gradient across the bottom substrate, the results can show the behavior of temperature increase as time after the laser radiation was applied to the sample. The results of the measured temperature profiles in Fig. 11 show that the temperature at the interface between the bottom substrate and the ceramic plate reached to 247.5°C and 280.7°C after 6 s at the laser power of 60 W and 70W and then 305.4°C and 338.2°C after 25 s respectively. The rate of temperature increase decreases as time. We have shown in our previous work that the laser induced temperature rise is typically exponential behavior [27]. After 300 s from the onset of the laser irradiation on the sample, the temperature was 317.4°C and 367.0°C respectively. These results indicate that the high strength within the sintered Ag layer and bonding between the nano-Ag layer and the Cu films may be from the effect of the fast heating rate in the laser assisted sintering process which has been shown to enhance the formation and growth of the initial sintering necks between nano-Ag particles [28], and then uniform networks of Ag structures are formed. The fast sintering process can also facilitate the bonding between the Ag particles and Cu films. The reason is that the short laser irradiation time can reduce oxidation of the Cu films during the sintering process. As a result, the bonding strength between the nano-Ag layer and the Cu films may be enhanced as compared with the samples sintered on hotplate. The high sintering temperature which is above the 317°C at the laser power of 60 W or 367°Cin the case of 70 W after 30 seconds of laser irradiation, would accelerate the Ostwald ripening of the Ag network in the sintered material [29], and thus strengthening the nano-Ag joint between the silicon substrates.

IV. Conclusions

A laser-assisted nano-Ag sintering process for die-attach applications has been studied in this work. It has been shown that fast sintering (bonding) can be realized within 1 minute. With the increase of laser irradiation time and power, coarsened networks of Ag structures would form. When the load is increased in the sintering process, the microstructures of the nano-Ag layer are densified. The shear strength of the samples produced using laser irradiation time between 2 min and 5 min was comparable and even higher than the samples sintered on hotplate for 80 min. Most of the samples sintered by laser irradiation showed mixed fracture mode: within the sintered Ag layer and at the interface of the sintered Ag layer and the Cu films. With the increase of laser power and sintering time, the bonding strength within the sintered Ag layer and between Ag and Cu films was enhanced in the laser sintering process, resulting from the effects of fast heating rate, high sintering temperature and short sintering time in the laser-assisted nano-Ag sintering method as compared with the hotplate based approach.

ACKNOWLEDGMENT

The laser sintering work was carried out at Heriot-Watt University. The work on shear test and cross-sectioning was performed at Harbin Institute of Technology and partially supported by the National Science Foundation of China (No. 51375003). Wei Liu was a visiting scholar at Heriot-Watt University supported by a scholarship from the China Scholarship Council (CSC).

References

[1] Z. T. Wang, W. Liu, C. Q. Wang, "Recent progress in ohmic contacts to silicon carbide for high-temperature applications," J. Electron. Mater. vol. 45, no.1, pp. 267-284, Jan. 2016.

[2] R. S. Okojie, D. Lukco, V. Nguyen, E. Savrun, "4H-SiC Piezoresistive pressure sensors at 800 °C with observed sensitivity recovery," IEEE Electr. Device L., vol. 36, no.2, pp. 174-176, Feb. 2015.

[3] Z. Zhang, G. Q. Lu, "Pressure-assisted low-temperature sintering of silver paste as an alternative die-attach solution to solder reflow," IEEE Trans. Electron. Packag. Manuf., vol.25, no.4, pp. 279-283, Oct. 2002.

[4] L. Jiang, T.G. Lei; K. D. T. Ngo, G. Q. Lu, S. Luo, "Evaluation of thermal cycling reliability of sintered nanosilver versus soldered joints by curvature measurement," IEEE Trans. Compon. Pack. Manuf. Technol., vol.4, no.5, pp. 751-761, May 2014.

[5] J. G. Bai, J. N. Calata, G. Q. Lu, "Processing and characterization of nanosilver pastes for die-attaching SiC devices," IEEE Trans. Electron. Packag. Manuf., vol.30, no.4, pp. 241-245, Oct. 2007.

[6] Y. F. Kong, X. Li, Y. H. Mei, G. Q. Lu, "Effects of die-attach material and ambient temperature on properties of high-power COB blue LED module," IEEE Trans. Electron Devices, vol.62, no. 7, pp. 2251-2256, Jul. 2015.

[7] L.A. Navarro, X. Perpiñà, P. Godignon, J. Montserrat, V. Banu, M. Vellvehi, X. Jordà, "Thermomechanical assessment of die-attach materials for wide bandgap semiconductor devices and harsh environment applications," IEEE Trans. Power Electron., vol.29, no.5, pp. 2261- 2271, May 2014.

[8] F. L. Henaff, S. Azzopardi, E. Woirgard, T. Youssef, S. Bontemps, J. Joguet, "Lifetime evaluation of nanoscale silver sintered power modules for automotive application based on experiments and finite-element modeling," IEEE Trans. Device Mater. Reliab., vol.15, no.3, pp. 326 - 334, Sept. 2015.

[9] G. Chen, Y. Cao, Y. Mei, D. Han, G. Q. Lu, X. Chen, "Pressure-assisted low-temperature sintering of nanosilver paste for 5x5 mm^2 chip

attachment," IEEE Trans. Compon. Pack. Manuf. Technol., vol.2, no.11, pp. 1759-1767, Nov. 2012.
[10] J. Kahler, N. Heuck, A.Stranz, A. Waag, E. Peiner, "Pick-and-place silver sintering die attach of small-area chips," IEEE Trans. Compon. Pack. Manuf. Technol., vol.2, no.2, pp. 199 -207, Feb. 2012.
[11] H. Li, H. Jing, Y. Han, "Interface evolution analysis of graded thermoelectric materials joined by low temperature sintering of nano-silver paste," J. Alloy. Compd., vol. 659, pp. 95-100, Feb. 2016
[12] K.S. Siow, "Mechanical properties of nano-silver joints as die attach materials," J. Alloy. Compd., vol. 514, pp. 6-19, Feb. 2012.
[13] N.B. Bell, C.B. DiAntonio, D.B. Dimos, "Development of conductivity in low conversion temperature silver pastes via addition of nanoparticles," J. Mater. Res., vol. 17, pp. 2423–2432, Sept. 2002.
[14] M. Kuramoto, T. Kunimune, S. Ogawa, M. Niwa, K. S. Kim, K. Suganuma, "Low-temperature and pressureless Ag–Ag direct bonding for light emitting diode die-attachment," IEEE Trans. Compon. Pack. Manuf. Technol., vol.2, no.4, pp. 548 - 552, Apr. 2012.
[15] Y. Tang, W. He, S.X. Wang, Z. H. Tao, Z.H. Tao, L. J. Cheng, "New insight into the size-controlled synthesis of silver nanoparticles and its superiority in room temperature sintering", Crystengcomm, Vol. 16, no. 21, pp. 4431-4440, Feb. 2014.
[16] R. Cruz; J. A. C. Ranita, J. Macaira, F. Ribeiro, A. M. B. Silva, J. M. Oliveira, M. H. F. V. Fernandes, H. A. Ribeiro, J. G. Mendes, A. Mendes, "Glass–glass laser-assisted glass frit bonding," IEEE Trans. Compon. Pack. Manuf. Technol., vol.2, no.12, pp. 1949 - 1956, Dec. 2012.
[17] X. Jiang, C. Wang, W. Liu, "A laser-assisted bonding method using a liquid crystal polymer film for MEMS and sensor packaging," IEEE Trans. Compon. Pack. Manuf. Technol., vol.5, no.5, pp. 583 - 591, May 2015.
[18] A. A. Tseng, J. S. Park, "Using transmission laser bonding technique for line bonding in microsystem packaging," IEEE Trans. Electron. Packag. Manuf., vol. 29, no. 4, pp. 308 - 318, Oct. 2006.
[19] L. Yang; W. Liu; C.Q. Wang; Y. H. Tian, "Surface-tension-driven self-assembly of 3-D microcomponents by using laser reflow soldering and wire limiting mechanisms," IEEE Trans. Compon. Pack. Manuf. Technol., vol.3, no.1, pp. 168 - 176, Jan. 2015.
[20] D. W. Tian, C. Q. Wang, Y. H. Tian, "modeling of micropitch shift of a magnetoelectrical sensor during laser solder ball bonding process," IEEE Trans. Adv. Packag., vol.32, no.1, pp. 136 - 145, Feb. 2015.
[21] C. J. Hyun, R. Kyongtae, P. Kyunghoon, S. J. Moon, "Thermal conductivity estimation of inkjet-printed silver nanoparticle ink during continuous wave laser sintering," Int. J. Heat Mass Transf., Vol.85, pp. 904-909, Jun. 2015
[22] K. An, S. Hong, S. Han, H. Lee, J. Yeo, S. H. Ko, "Selective sintering of metal nanoparticle ink for maskless fabrication of an electrode micropattern using a spatially modulated laser beam by a digital micromirror device," ACS Appl. Mater. Interfaces, vol.6, no.4, pp. 2786-2790, Feb. 2014.
[23] D.G. Lee, D.K. Kim, Y.J. Moon, S.J. Moon, "Estimation of the properties of silver nanoparticle ink during laser sintering via in-situ electrical resistance measurement," J. Nanosci. Nanotechnol., vol. 13, no. 9, pp. 5982-5987, Sep. 2013
[24] D.G. Lee, D.K. Kim, Y.J. Moon, S.J. Moon, "Effect of laser-induced temperature field on the characteristics of laser-sintered silver nanoparticle ink," Nanotechnology, vol.24, no. 26, pp. 265702, Jul. 2013.
[25] C.H. Wang, “Laser assisted polymer joining methods for photonic devices,” in Laser Growth and Processing of Photonic Devices, N. A. Vainos, Ed. Woodhead Publishing (Cambridege, UK), 2012, pp. 269-284.
[26] Y. S. Lee, C. Yun, K. H. Kim, W. H. Kim, S-W Jeon, J. K. Lee, and J. P. Kim, “Laser-sintered silver nanoparticles as a die adhesive layer for high-power light-emitting diodes”, IEEE T. Comp. Pack. Man., vol.4, no.7 pp. 1119-1124, July. 2014.
[27] Y. Liu, J. Zeng, and C. Wang, “Accurate temperature monitoring in laser-assisted polymer bonding for MEMS packaging using an embedded microsensor array,” J. Microelectromech. Syst., vol. 19, no. 4, pp. 903-910, Aug. 2010.
[28] P. Peng, A. Hu, Y. Zhou, " Laser sintering of silver nanoparticle thin films: microstructure and optical properties," Appl. Phys. A-Mater. Sci. Process., vol.108, no. 3, pp. 685-691, Sep. 2012.
[29] R. Cauchois, M. Saadaoui, J. Legeleux, T. Malia, B. D. Bonvalot, "Wire-bonding on inkjet-printed silver pads reinforced by electroless plating for chip on flexible board packages," ESTC 2010. Electronics System Integration Technology Conference, Berlin, Germany, Sep 2010.

TABLE I. SHEAR STRENGTH OF SAMPLES SINTERED BY DIFFERENT METHODS AND PARAMETERS (MPa)

Hot plate, 0.1 kg load		Laser, 0.1 kg load			Laser 0.5 kg load	
260℃	285℃	60 W, 2 min	60 W, 5 min	70 W, 1 min	70 W, 1 min	70 W, 5min
4.79	4.64	4.43	5.11	1.89	2.08	5.54

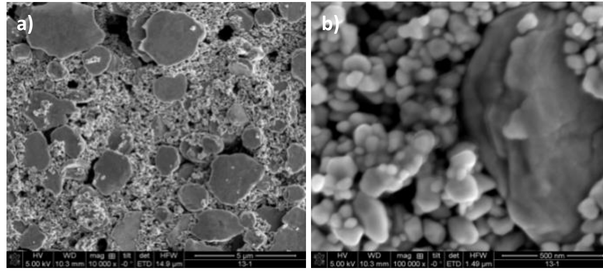

Fig. 1 SEM pictures of the nano-Ag paste after heating at 110°C for 5 minutes, (a) 10 000X, b) 100 000X

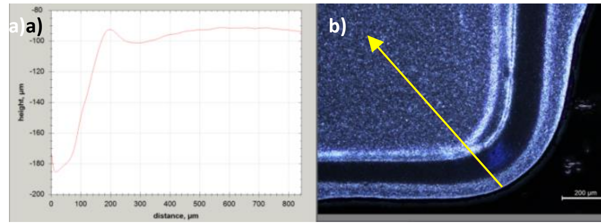

Fig. 2 Thickness profile of the printed nano-Ag paste: (a) thickness profile and (b) test location and direction

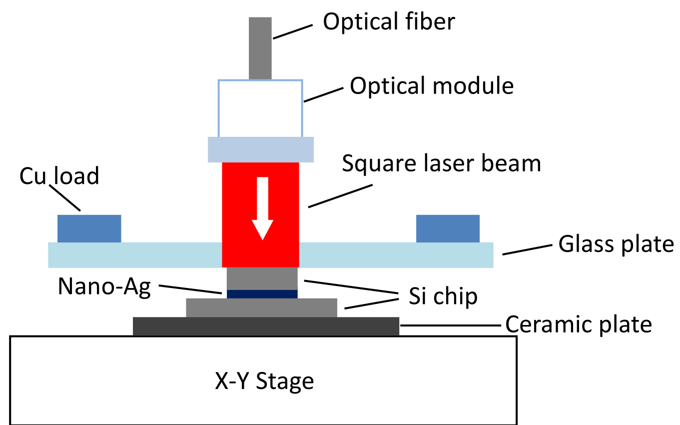

Fig. 3 A schematic of the laser-assisted sintering setup.

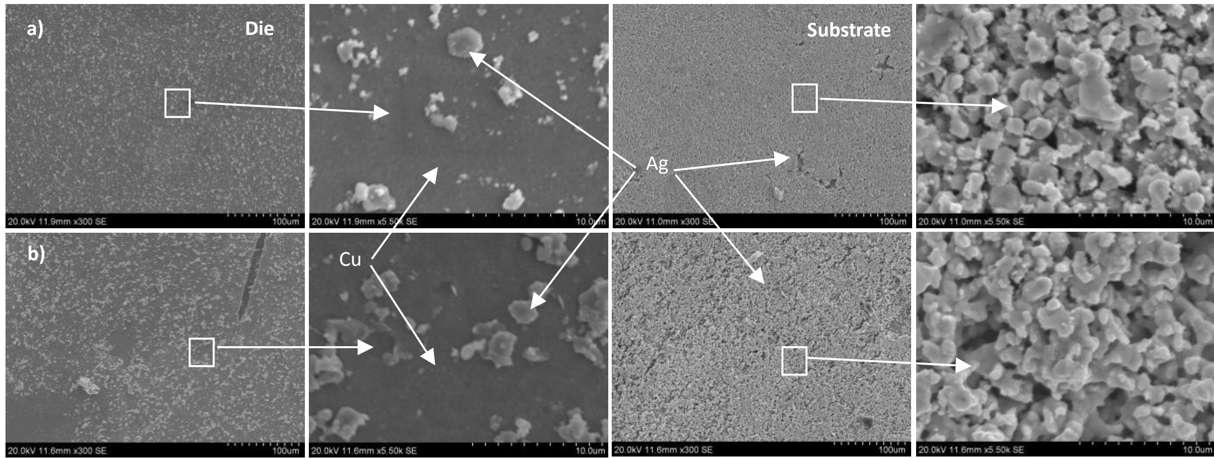

Fig.4 Fracture surfaces of samples sintered by hot plate at different final stage temperatures, (a) 260°C and (b) 285°C

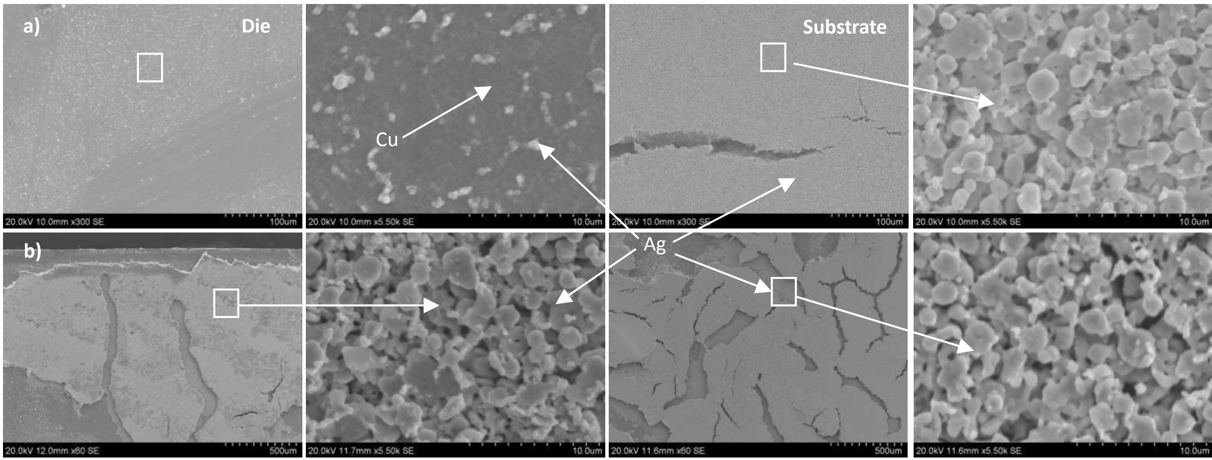

Fig. 5 Fracture surfaces of laser sintered samples using 60 W of laser power and 0.1 kg of load, (a) 2 min and (b) 5min

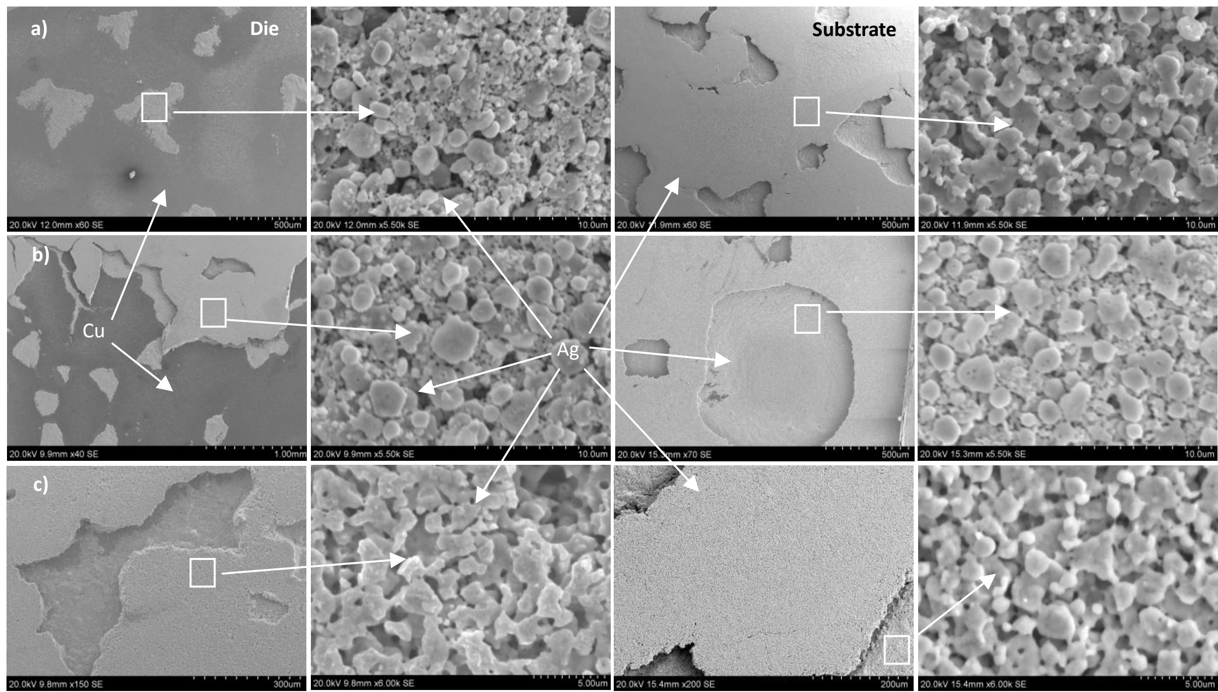

Fig. 6 Fracture surfaces of samples sintered by 70 W of laser irradiation under different loads and times. (a) 0.1 kg and 1 min, (b) 0.5 kg and 1 min, and (c) 0.5 kg and 5min.

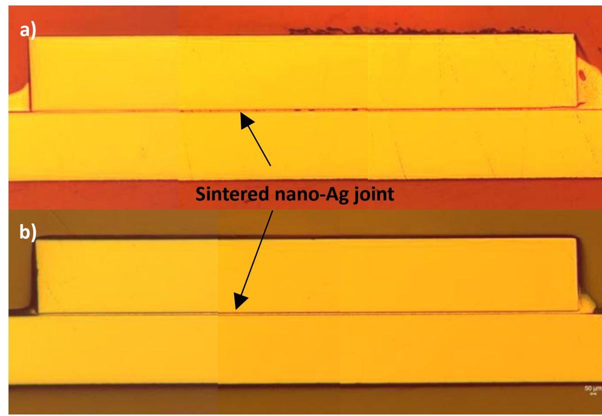

Fig. 7 Cross-sections of samples sintered by hotplate (a) and laser (b) based methods.

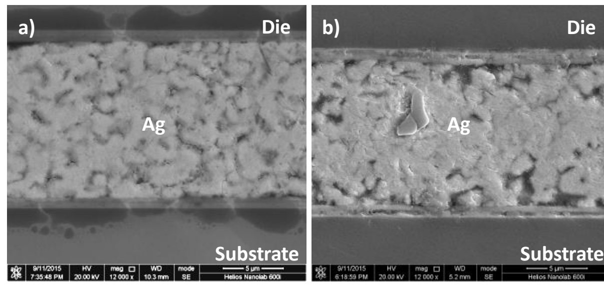

Fig. 8 Cross-sections of samples sintered on hotplate at different final stage temperatures: (a) 260°C and (b) 285°C.

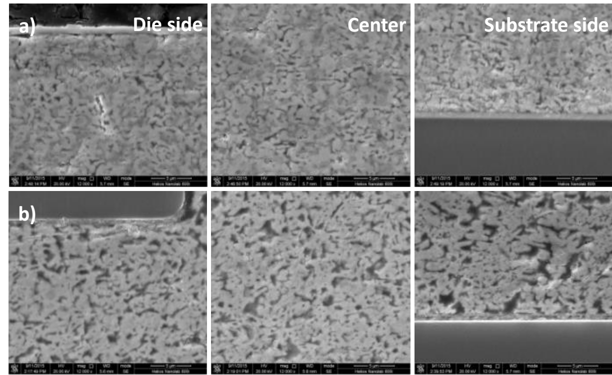

Fig. 9 Cross-sections of samples sintered using 60W of laser irradiation and 0.1 kg of load, (a) 2 min and (b) 5 min.

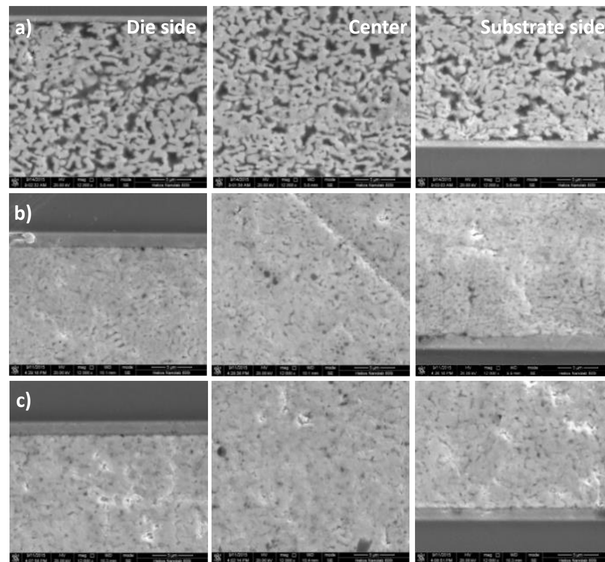

Fig. 10 Cross-sections of samples sintered using 70 W of laser power and different loads and irradiation times. (a) 0.1 kg and 1 min, (b) 0.5 kg, 1 min, and (c) 0.5 kg, 5 min.

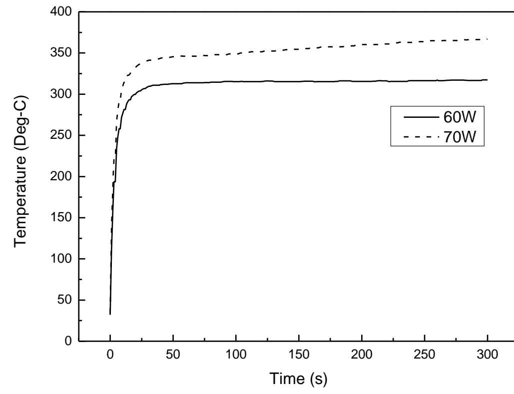

Fig. 11 Temperature profiles of the laser heating effect obtained using a thermocouple placed underneath the bottom silicon substrate.